Non-axisymmetric flow in a rotating cylinder : Incompressible and compressible fluids

AUTHOR(S):

NAKAGAWA, KEIZO; TAKEDA, HIDENORI; MATSUDA, TAKUYA

数理解析研究所講究録
476巻 1983年 16-52

16

Non-axisymmetric flow in a rotating cylinder

— Incompressible and compressible fluids —

By KEIZO NAKAGAWA, HIDENORI TAKEDA and TAKUYA MATSUDA

Department of Aeronautical Engineering, Kyoto University,
Kyoto, Japan

Analytic and numerical calculations on non-axisymmetric flows in a rotating cylinder are performed for both compressible and incompressible fluids. Non-axisymmetric character is induced by the bottom shape such as a sloping flat bottom or an off-axial paraboroid. In the case of the incompressible fluid the flow field is independent of the axial coordinate due to the Taylor-Proudman theorem, and the phenomenon which is called westward intensification is observed. In the compressible case, on the other hand, flowlines are confined to the surfaces whose radial coordinates are constant, while non-axisymmetric weak axial motion is induced by the bottom slope.

1. Introduction

Dynamics of rotating fluid has been developed to understand an oceanic or an atmospheric flow (see Greenspan 1968) and a flow in a gas centrifuge to separate uranium isotopes (see Soubbaramayer 1979). In the former case the fluid is usually considered as incompressible and a Coriolis force plays more dominant role than a centrifugal force, while in the latter compressibility and the centrifugal force are significant. Matsuda, Sakurai and Takeda (1975) showed, however, that the nature of a compressible flow in a rapidly rotating cylinder is similer to the corresponding incompressible one, as long as the flow field is axisymmetric and the cylinder wall is thermally conducting. In the series of papers, Matsuda, Hashimoto and Takeda (1978a, 1978b) clarified that the properties of a compressible fluid are very different from the incompressible counterparts if a cylinder wall is thermally insulated. In the present paper non-axisymmetric flows are investigated to find possible differences between incompressible and compressible fluids.

Pedlosky and Greenspan (1967) and Beardsley (1969) considered the slow, viscously driven motion of an incompressible homogenous fluid in a rotating cylinder with a sloping flat bottom. They studied the steady motion produced in the cylinder when the upper surface normal to the cylinder axis rotates at a different rate than the rest of the container. They showed that the presence of the bottom slope inhibits a geostrophic wind of order unity and introduced a non-symmetric side wall boundary layer. Kuo and Veronis(1971) studied a flow induced by a source/sink in a pie-shaped basin with free surface and obtain a similar flow pattern

as Pedlosky and Greenspan (1967).

These studies were performed to simulate the large-scale oceanic circulation. In a simple model of the ocean a hydrostatic balance and an incompressible homogenous fluid are assumed. To treat the local motion in the ocean, we consider two-dimensiona flow on a rotating large sphere. Then the following coservation law of potential vorticity holds (see Charney 1973):

$$\frac{D}{Dt}\left[\frac{f+\zeta}{h}\right] = 0 , \tag{1.1}$$

where D/Dt is the time derivative following the motion of a fluid particle, $f = 2\Omega \sin\psi$ (Ω: angular velocity of the earth and ψ: latitude) is Coriolis parameter, ζ is the relative vorticity component normal to the surface of the earth, and h is the depth of the fluid. From this relation we can simulate the β-effect (the effect due to the latitudinal variation of the Coriolis parameter) by the variation in the depth of the fluid. In the above works, i.e. Pedlosky & Greenspan (1967), Beardsley (1969), and Kuo & Veronis (1971), a boundary layer is found to be formed at the western side wall of the container. The flow in the boundary layer is intense and this phenomenon is a model for a westward intensification in an oceanography, such as the Gulf Stream or the Kuroshio Current.

These two models of Pedlosky & Greenspan (1967) and Kuo & Veronis (1971) are united in a concept of topology of a geostrophic contour, which is a line of equal depth of fluid. In the axisymmetric flow with free surface, for example, all geostrophic contours are closed. In this case the O(1)

geostrophic wind can blow along geostrophic contours. When none of geostrophic contours are closed as in the case of Pedlosky & Greenspan and Kuo & Veronis, the O(1) geostrophic wind is inhibited and a boundary layer is formed along the western boundary. In §2 an intermediate case in which some of geostrophic contours are open is considered, and a gradual transition from one to another is studied. Such an intermediate condition is realized in a rotating cylinder whose bottom shape is an off-axial paraboroid and whose upper surface rotates faster or slower.

Now turning to the compressible fluid, the situation is very different. Due to the compressibility and the strong centrifugal force a stable stratification is made along a radial coordinate. Therefore flow is confined to a concentric anulus even if an axisymmetric condition is dropped. We focus our attention on the non-axisymmetric flow produced by a sloping bottom in §3.

2. Incompressible fluid

2.1 Basic equations

Consider the fluid in the circular cylinder rotating about the vertical z-axis with a uniform angular velocity. The upper surface rotates steadily with an angular velocity $\Omega+\Delta\Omega$, while the rest of the cylinder rotates at Ω(figure 1.). The steady, linealized, non-dimensional equations of motion and continuity for a viscous incompressible fluid written in terms of the

rotating frame of reference are

$$2\mathbb{k} \times \mathbb{q} = -\nabla p + E \Delta \mathbb{q} \quad , \tag{2.1}$$

$$\nabla . \mathbb{q} = 0 \, , \tag{2.2}$$

where $\mathbb{q}$ is the velocity vector, $\mathbb{k}$ is the vertical unit vector, $E = \nu / \Omega L^2$ is the Ekman number and ν is the kinematic viscosity. The lengths are scaled in terms of the radius L of the cylinder. The pressure is scaled by $\rho\Omega LU$ where ρ is the density and $U = |\Delta\Omega| L$ is a characteristic velocity.

The top cover is flat and normal to the z-axis at $z = H_0$, while the bottom shape is expressed in terms of the following covergent series:

$$z = H(r,\theta) = F \sum_{m=0}^{\infty} h_m(r) \cdot e^{im\theta} \, , \tag{2.3}$$

where it is assumed that $F \ll 1$ and the bottom surface is sufficiently smooth. The boundary conditions on $\mathbb{q}$ are $\mathbb{q} = (0,r,0)$ at $z = H_0$ and $\mathbb{q} = \mathbb{0}$ at $r = 1$ and $z = H(r,\theta)$.

Since we have an interest in the interior flow, we treat implicitly the Ekman layers developed on the top and bottom surfaces. The Ekman layer suction is then expressed as a compatibility condition, on the interior velocity components u, v and w, just outside the upper Ekman layer:

$$w = \frac{1}{2} E^{\frac{1}{2}} (2 - \zeta) \qquad \text{at} \quad z = H_0 \, , \tag{2.4}$$

where ζ is the z-component of the vorticity vector ω. The Ekman compatibility condition also holds on a slightly inclined bottom surface, and we have

$$(\xi \cdot n^*) = \frac{1}{2} E_*^{\frac{1}{2}} (\omega \cdot n^*) \qquad \text{at } z = H(r,\theta), \tag{2.5}$$

where n^* is a vector normal to the bottom surface, and the modified Ekman number E_* is used because of the inclination of the bottom surface. Since we assume that the angle between the normal vector n^* and the rotation axis is on the order of F, E_* is nearly equal to E for $F \ll 1$. The normal vector n^* is expressed in terms of cylindrical coordinate (r,θ,z) :

$$n^* = \left(-F\sum_{m=0}^{\infty} \frac{dh_m}{dr} e^{im\theta},\ -F\sum_{m=0}^{\infty} \frac{h_m}{r} im e^{im\theta},\ 1\right). \tag{2.6}$$

Introducing (2.6) into (2.5) and noting $F \ll 1$, we obtain

$$w = F\left(u\sum_{m=0}^{\infty} \frac{dh_m}{dr} e^{im\theta} + v\sum_{m=0}^{\infty} \frac{h_m}{r} im e^{im\theta}\right) + \frac{1}{2} E^{\frac{1}{2}} \zeta \qquad \text{at } z = H(r,\theta). \tag{2.7}$$

The interior dynamics are constrained by the Taylor-Proudman theorem. The interior velocity components are independent of z to O(E), therefore the fluid motion is columnar. Equating vertical velocities in (2.4) and (2.7) we get

$$E^{\frac{1}{2}} \zeta + F\left(u\sum_{m=0}^{\infty} \frac{dh_m}{dr} e^{im\theta} + v\sum_{m=0}^{\infty} \frac{h_m}{r} im e^{im\theta}\right) = E^{\frac{1}{2}}. \tag{2.8}$$

The interior flow satisfys the geostrophic and hydrostatic relations : $2\,\mathbb{k}\times\mathbf{q} = -\nabla p$, therefore we can eliminate u and v from (2.8) favouring p to yield

$$\epsilon\,\Delta p - \frac{1}{r}\frac{\partial p}{\partial\theta}\sum_{m=0}^{\infty}\frac{dh_m}{dr}e^{im\theta} + \frac{i}{r}\frac{\partial p}{\partial r}\sum_{m=0}^{\infty} m h_m e^{im\theta} = 2\epsilon \,, \tag{2.9}$$

where $\epsilon = E^{\frac{1}{2}} / F$.

For instance we consider the cylinder whose bottom shape is an off-axial paraboroid given as

$$H(r,\theta) = F\left(-\frac{1}{2}r^2 + b\,r\cos\theta\right) , \tag{2.10}$$

where b is a radial distance between z-axis and the apex of the paraboroid. Substituting (2.10) into (2.9), we obtain the basic equation to be solved :

$$\epsilon\,\Delta p + \left(1 - \frac{b}{r}\cos\theta\right)\frac{\partial p}{\partial\theta} - b\sin\theta\,\frac{\partial p}{\partial r} = 2\epsilon \,. \tag{2.11}$$

This equation is made simpler in the rotating frame whose axis is a vertical line through the apex of the bottom, i.e. $r = b$, $\theta = 0$. In this frame (R,ϕ,z), (2.11) is written as

$$\epsilon\,\Delta p + \frac{\partial p}{\partial\phi} = 2\epsilon \,, \tag{2.12}$$

which is identical to the equation derived by Kuo & Veronis (1971). From the geostrophic balance equations pressure field p can be considered as a stream function , and therefore the boundary condition for p at the side wall should be p = 0 . In the present paper we assume $E^{\frac{1}{2}} \ll F \ll 1$, so we have $\varepsilon \ll 1$. This condition is the same as Stommel's (1948) model of the wind-driven oceanic circulation.

Pedlosky & Greenspan (1967) considered a sloping flat bottom, that is

$$H(r,\theta) = \tan F \cdot x \approx F r \cos\theta \quad , \tag{2.13}$$

where F is a small angle of the slope. In this case the basic equation reduces to

$$\epsilon \Delta p + \frac{\cos\theta}{r}\frac{\partial p}{\partial \theta} + \sin\theta \frac{\partial p}{\partial r} = 2\epsilon \, . \tag{2.14}$$

2.2 Solution in the case of b > 1

If $\varepsilon \ll 1$ and $b > 1$, (2.11) or (2.12) can be solved by the method of singular perturbation (Cole 1968) . Neglecting $\varepsilon\Delta p$ term of (2.12) , a solution in an inner region is obtained as follows:

$$p_I = 2\epsilon\phi + f(R) \, , \tag{2.15}$$

where f(R) is an arbitrary function of R and is determined by the boundary condition. Neverthless there is not enough arbitrariness to satisfy the boundary condition completely along the side wall. Hence proceeding in the usual manner, we stretch the radial coordinate near r = 1 as

$$1 - r = \epsilon \zeta \,, \tag{2.16}$$

and can reduce (2.11) to

$$\frac{\partial^2 \hat{p}}{\partial \zeta^2} + b \sin\theta \, \frac{\partial \hat{p}}{\partial \zeta} = 0 \,, \tag{2.17}$$

where $\hat{p}$ is a boundary layer correction. The boundary conditions for $\hat{p}$ are

$$\begin{aligned} &\hat{p} = - p_I (r=1) && \text{at} \quad \zeta = 0 \,, \\ &\hat{p} \longrightarrow 0 && \text{when} \quad \zeta \longrightarrow \infty \,. \end{aligned} \tag{2.18}$$

The solution of (2.17) satisfying (2.18) is

$$\hat{p} = - p_I (r=1) \cdot e^{-b \sin\theta \cdot \zeta} \qquad (0 < \theta < \pi) \,. \tag{2.19}$$

This boundary layer can be called the Stommel boundary layer, since (2.11) is essentially same as the Stommel's equation to

explain the westward intensification in an oceanography (Stommel 1948). This boundary layer exists only for $0 < \theta < \pi$, that is along the west coast. Satisfying the boundary condition $p_I = 0$ at $r = 1$ and $\pi \leqq \theta \leqq 2\pi$, $f(R)$ is determined and the inner solution p_I is expressed in the original frame (r,θ,z) as

$$p_I = 2\epsilon \left[-\tan^{-1}\left(\frac{r\sin\theta}{b - r\cos\theta}\right) - \tan^{-1}\left\{\frac{(4b^2 - (1-r^2+2br\cos\theta)^2)^{\frac{1}{2}}}{2b^2 - (1-r^2+2br\cos\theta)}\right\}\right] \qquad (2.20)$$

The thickness of the Stommel boundary layer in this problem is $\epsilon / \sin\theta$, which diverges as $\theta \to 0, \pi$. In the region near $\theta = 0$ and π, the boundary layer approximation is not valid. In figure 2 an analytic solution and a numerical solution computed by a successive over-relaxation method are shown and compared in the case of $\epsilon = 0.01$ and $b = 1.5$.

For $0 < b < 1$ the inner solution (2.15) is not valid any longer, for the term $2\epsilon\phi$ dose not satisfy a periodic condition when ϕ increases from 0 to 2π. In the Kuo & veronis' problem or our problem for $b > 1$, the range of ϕ is limited to $0 < \phi_{min} < \phi < \phi_{max} < 2\pi$ and any difficulty does not occur.

2.3 Solution in the case of $0 < b \ll 1$

A simple analytic solution of (2.11) for $0 < b < 1$ could not be obtained. But in the case of $b \ll 1$ we can get an analytic solution by expanding the pressure p in terms of b, i.e.

$$p = p_0(r) + b \cdot p_1(r,\theta) + b^2 \cdot p_2(r,\theta) + \cdots \qquad (2.21)$$

The substitution of (2.21) into (2.11) leads to the following zeroth and m-th order equations:

$$\frac{1}{r}\frac{d}{dr}\left(r\frac{dp_0}{dr}\right) = 2, \tag{2.22}$$

$$\epsilon \Delta p_m + \frac{\partial p_m}{\partial \theta} = \frac{\cos\theta}{r}\frac{\partial p_{m-1}}{\partial \theta} + \sin\theta \frac{\partial p_{m-1}}{\partial r} . \tag{2.23}$$

$$(m = 1, 2, \cdots)$$

The boundary conditions for these equations are $p_0 = p_m = 0$ on $r = 1$.

The zoroth order solution should be axisymmetric and is easily obtained :

$$p_0 = \frac{1}{2}(r^2 - 1). \tag{2.24}$$

The first order equation, using (2.24), is

$$\epsilon \Delta p_1 + \frac{\partial p_1}{\partial \theta} = r \sin\theta . \tag{2.25}$$

A particular solution of (2.25) is

$$p_{1p} = - r \cos\theta . \tag{2.26}$$

To solve the homogenous problem, the pressure field p_1 is expanded in a Fourier series :

$$p_1 = \sum_{n=0}^{\infty} \{ C_n(r) \cdot \cos n\theta + S_n(r) \cdot \sin n\theta \} . \qquad (2.27)$$

Substituting (2.27) into the homogenous equation of (2.25) and introducing the function $X_n = C_n + i S_n$ where $i = \sqrt{-1}$, the Fourier coefficients should satisfy the following equation :

$$\frac{1}{r}\frac{d}{dr}\left(r \frac{dX_n}{dr} \right) - \left(\frac{in}{\epsilon} + \frac{n^2}{r^2} \right) X_n = 0 , \qquad (2.28)$$

with the Bessel function solution given by

$$X_n = J_n \left(\sqrt{\frac{n}{\epsilon}} \cdot e^{-\frac{\pi}{4} i} \cdot r \right) . \qquad (2.29)$$

The total solution of (2.25), together with the boundary condition, is

$$p_1 = -r\cos\theta + \frac{Re\left[J_1 \left(e^{-\frac{\pi}{4} i} \, r / \epsilon^{\frac{1}{2}} \right) \right]}{Re\left[J_1 \left(e^{-\frac{\pi}{4} i} / \epsilon^{\frac{1}{2}} \right) \right]} \cos\theta , \qquad (2.30)$$

where $Re[\alpha]$ indicates a real part of α.

Near the side boundary, that is $r \approx 1$, $r/\epsilon^{\frac{1}{2}}$ is a considerably large value, and from the asymptotic series of a first order Bessel function we can estimate the boundary layer contribution.

$$\begin{aligned} \mathrm{Re}\left[J_1 (e^{-\frac{\pi}{4} i} r / \epsilon^{\frac{1}{2}}) \right] &\sim \sqrt{\frac{\epsilon^{\frac{1}{2}}}{2\pi r}} \; e^{\frac{r}{\sqrt{2}\,\epsilon^{\frac{1}{2}}}} \\ &\sim \sqrt{\frac{1}{2\pi (\epsilon^{-\frac{1}{2}} - \eta)}} \; e^{\frac{1}{\sqrt{2}} (\epsilon^{-\frac{1}{2}} - \eta)} , \end{aligned} \tag{2.31}$$

where η is a stretched coordinate of r as

$$1 - r = \epsilon^{\frac{1}{2}} \eta . \tag{2.32}$$

The equation (2.31) shows the existence of the boundary layer with thickness of $\epsilon^{\frac{1}{2}}$ along the side wall. Therefore the first and second term of the solution (2.30) correspond to the inner solution and the boundary layer component respectively.

To clarify the structure of the boundary layer by simpler functions and to proceed to higher order solutions easily, we use the boundary layer equation written by the stretched coordinate η given by (2.32) :

$$\frac{\partial^2 \hat{p}_1}{\partial \eta^2} + \frac{\partial \hat{p}_1}{\partial \theta} = 0 , \tag{2.33}$$

where $\hat{p}_1$ is a boundary layer correction with boundary conditions as

$$\begin{aligned} \hat{p}_1 &= - p_{1F} (r = 1) \qquad \text{at} \quad \eta = 0 , \\ \hat{p}_1 &\longrightarrow 0 \qquad\qquad \text{when} \quad \eta \longrightarrow \infty . \end{aligned} \tag{2.34}$$

Thus the approximate solution of (2.25) is given by

$$P_1 = P_{1P} + \hat{P}_1$$
$$= -r\cos\theta + e^{-\frac{\eta}{\sqrt{2}}} \cos\left(\theta + \frac{\eta}{\sqrt{2}}\right) . \qquad (2.35)$$

The right hand side of (2.23) for m = 2 has only boundary layer components, and therefore it is shown that higher order solutions than the first order give the variations only in a bounbary layer and a small constant of $O(b^m)$ in the inner region. For this reason the flow pattern in the inner core is determined by the first two terms of the expansion with respect to b. Omitting the side buondary layer contribution, the solution in the inner region is

$$P_I = \frac{1}{2}(r^2-1) - br\cos\theta$$
$$= \frac{1}{2}\left\{ (x-b)^2 + y^2 - (1+b^2) \right\} , \qquad (2.36)$$

where $x = r\cos\theta$, $y = r\sin\theta$, and the constant terms arising from the higher order contributions are neglected. This solution indicates that the flow pattern is axisymmetric about the summit of the bottom. It can be obviously shown that a necessary condition for the convergence of the series (2.21) is $b < \varepsilon^{\frac{1}{2}}$. Both analytic and numerical solutions for b = 0.05 and ε = 0.01 are shown in figure 3.

2.4 Results

In the axisymmetric case, i.e. $b = 0$, the first term, $\varepsilon\Delta p$, of (2.11) balances with the right hand side, 2ε, and the $O(1)$ axisymmetric geostrophic wind can blow. Introducing small b, the axisymmetric flow pattern shifts only by b and $\varepsilon^{\frac{1}{2}}$-layer is formed along the side wall. The order of magnitude of pressure field still remains $O(1)$. On the other hand, for $b > 1$ the solution (2.15) clearly shows that p is $O(\varepsilon)$, which results from the fact that the second term of (2.12) balances with the 2ε term. In this case the Stommel boundary layer of thickness ε is developed along the western boundary. In the case of $b \leq 1$, an intermediate situation between the above two cases is expected. Since we could not solve the case of $b \leq 1$ analytically, we give numerical solutions for $b = 0.5$, 0.7 and 0.9 in figures 4, 5 and 6, and it seems to come up to the above expectation. In figure 7 the locus of the point of the minimum pressure is drawn, and the transition of the flow pattern with varying b can be seen.

Pedlosky & Greenspan's equation (2.14) can be easily solved by the same method as the case of $b > 1$ and is shown here.

$$p = \begin{cases} 2\epsilon \left[y \left\{ 1 - 2e^{-\sin\theta \cdot (1-r)/\epsilon} \right\} + (1-x^2)^{\frac{1}{2}} \right] & (0 < \theta < \pi) \\ 2\epsilon \left[y + (1-x^2)^{\frac{1}{2}} \right] & (\pi \leq \theta \leq 2\pi) \end{cases} \tag{2.37}$$

which is also $O(\varepsilon)$.

These results are explained in terms of the geostrophic contour. If all geostrophic contours are closed such as $b = 0$ in (2.11), the flowlines are along geostrophic contours and the

magnitude of the flow is O(1). On the other hand, if none of geostrophic contours are closed as in the case of $b > 1$ in (2.11) or in the case of (2.14), there are no geostrophic winds of O(1). This is caused by the fact that velocity components should be independent of z and the change rate of the hight of fluid column should be $O(E^{\frac{1}{2}})$. The transition from the former case to the latter should be gradual. In the intermediate case such as $0 < b < 1$, some geostrophic contours are closed. The strength of the flow is between O(1) and $O(\varepsilon)$, and along the side wall the ε^n-layer $(1/2 < n < 1)$ seems to be formed.

3. Compressible fluid

3.1 Basic equations

Consider a gas in a cylinder rotating about a vertical axis. The mechanism to drive a steady flow is the same as that of an incompressible case, i.e. the top plate rotates with an angular velocity $\Omega + \Delta\Omega$ and other walls rotate at Ω. The angular velocity Ω is so high that the effect of the earth's gravity can be neglected. The non-dimensional linearized basic equations, governing the deviations in the fluid motion from the rigid rotation with angular velocity Ω and constant temperature T_0, are

$$\mathrm{div}\, \rho + G_0 r u = 0 , \qquad (3.1)$$

$$-2v + r\Gamma + \frac{1}{G_0}\frac{\partial p}{\partial r} = \frac{E}{\epsilon_R}\left[\mathcal{L}u + \frac{1}{3}\frac{\partial}{\partial r}(\operatorname{div}\mathbf{q}) - \frac{2}{r^2}\frac{\partial v}{\partial \theta}\right], \tag{3.2}$$

$$2u + \frac{1}{G_0 r}\frac{\partial p}{\partial \theta} = \frac{E}{\epsilon_R}\left[\mathcal{L}v + \frac{1}{3r}\frac{\partial}{\partial \theta}(\operatorname{div}\mathbf{q}) + \frac{2}{r^2}\frac{\partial u}{\partial \theta}\right], \tag{3.3}$$

$$\frac{1}{G_0}\frac{\partial p}{\partial z} = \frac{E}{\epsilon_R}\left[\Delta w + \frac{1}{3}\frac{\partial}{\partial z}(\operatorname{div}\mathbf{q})\right], \tag{3.4}$$

$$-4hru = \frac{E}{\epsilon_R}\Delta T, \tag{3.5}$$

$$p = \rho + T, \tag{3.6}$$

where

$$\operatorname{div}\mathbf{q} = \frac{1}{r}\frac{\partial}{\partial r}(ru) + \frac{1}{r}\frac{\partial v}{\partial \theta} + \frac{\partial w}{\partial z}, \tag{3.7}$$

$$\Delta = \frac{1}{r}\frac{\partial}{\partial r}\left(r\frac{\partial}{\partial r}\right) + \frac{1}{r^2}\frac{\partial^2}{\partial \theta^2} + \frac{\partial^2}{\partial z^2}, \qquad \mathcal{L} = \Delta - \frac{1}{r^2}, \tag{3.8}$$

$$G_0 = \frac{ML^2\Omega^2}{RT_0}, \qquad E = \frac{\nu}{\Omega L^2}, \qquad h = \frac{(\gamma-1)P_r G_0}{4\gamma}, \tag{3.9}$$

$$\epsilon_R = \exp\left\{\frac{1}{2}G_0(r^2-1)\right\} \tag{3.10}$$

Here $q_j = (u,v,w)$ is the velocity vector, M the mean molecular weight of the gas, R the universal gas constant, ν the kinematic

viscosity measured at the side wall and γ the ratio of specific heats. The non-dimensional parameter G_0 is the square of the rotational Mach number, E is the Ekman number, Pr is the Prandtl number and h is a parameter measuring the heat generation or absorption due to the radial fluid motion. In the above expression the velocity, temperature and position have been non-dimensionalized by $|\Delta\Omega|L$, T_0, and radius of the cylinder L, respectively. In this paper we assume that $E \ll 1$ and that G_0 and Pr are of order unity. The boundary conditions for the present problem are $q = 0$ and $T = 0$ on the side wall and the bottom, and $q = (0,r,0)$ and $T = 0$ on the top end.

In the inner core the radial velocity u is O(E) and physical variables are normalized as

$$u = E u_I \quad , \quad v = v_I \quad , \quad w = w_I \quad ,$$
$$T = T_I \quad , \quad P = P_I \quad , \quad \rho = \rho_I \quad , \tag{3.11}$$

where the suffix I refers to the main inner flow. Now all variables are expanded in Fourier series, e.g.

$$u_I = \sum_{m=0}^{\infty} u_m(r,z)\, e^{im\theta} \quad . \tag{3.12}$$

Substituting (3.11) and (3.12) into (3.1) to (3.6) and retaining only relevant terms, we have

$$\frac{\partial \bar{w}_0}{\partial z} + \sum_{m=1}^{\infty} \left(\frac{im}{r} v_m + \frac{\partial w_m}{\partial z} \right) e^{im\theta} = 0 \quad , \tag{3.13}$$

$$\sum_{m=0}^{\infty} \left(-2v_m + r T_m + \frac{1}{G_0} \frac{\partial p_m}{\partial r} \right) e^{im\theta} = 0 , \tag{3.14}$$

$$2u_0 + \sum_{m=1}^{\infty} \left(2u_m + \frac{im}{G_0 E r} p_m \right) e^{im\theta} = \frac{1}{\epsilon_R} \mathcal{L} \left(\sum_{m=0}^{\infty} v_m e^{im\theta} \right) , \tag{3.15}$$

$$\sum_{m=0}^{\infty} \frac{1}{G_0 E} \frac{\partial p_m}{\partial z} e^{im\theta} = \frac{1}{\epsilon_R} \Delta \left(\sum_{m=0}^{\infty} w_m e^{im\theta} \right) , \tag{3.16}$$

$$-4hr \sum_{m=0}^{\infty} u_m e^{im\theta} = \frac{1}{\epsilon_R} \Delta \left(\sum_{m=0}^{\infty} T_m e^{im\theta} \right) , \tag{3.17}$$

$$p_m = \rho_m + T_m . \tag{3.18}$$

We can separate the axisymmetric mode, i.e. m = 0 , and non-axisymmetric modes. Axisymmetric equations are

$$\frac{\partial w_0}{\partial z} = 0 , \tag{3.19}$$

$$-2v_0 + r T_0 + \frac{1}{G_0} \frac{\partial p_0}{\partial r} = 0 , \tag{3.20}$$

$$2u_0 = \frac{1}{\epsilon_R} \mathcal{L}_0 v_0 , \tag{3.21}$$

$$\frac{\partial p_0}{\partial z} = 0 , \tag{3.22}$$

$$-4hr u_0 = \frac{1}{\epsilon_R} \Delta_0 T_0 , \tag{3.23}$$

$$p_0 = \varsigma_0 + T_0 \ , \tag{3.24}$$

where

$$\Delta_0 = \frac{1}{r}\frac{\partial}{\partial r}\left(r\frac{\partial}{\partial r}\right) + \frac{\partial^2}{\partial z^2} \ , \qquad \mathcal{L}_0 = \Delta_0 - \frac{1}{r^2} \ . \tag{3.25}$$

Non-axisymmetric component of the pressure, p_m, should be O(E). Therefore, introducing $E\,p_m$ instead of p_m into (3.13) to (3.18) and dropping small terms, we can obtain the following non-axisymmetric part of the equations :

$$\frac{im}{r} v_m + \frac{\partial w_m}{\partial z} = 0 \ , \tag{3.26}$$

$$-2v_m + r T_m = 0 \ , \tag{3.27}$$

$$2u_m + \frac{im}{G_0 r} p_m = \frac{1}{\epsilon_R} \mathcal{L}_m v_m \ , \tag{3.28}$$

$$\frac{1}{G_0}\frac{\partial p_m}{\partial z} = \frac{1}{\epsilon_R} \Delta_m w_m \ , \tag{3.29}$$

$$-4hr u_m = \frac{1}{\epsilon_R} \Delta_m T_m \ , \tag{3.30}$$

$$0 = \varsigma_m + T_m \ , \tag{3.31}$$

$$(m = 1, 2, \cdots)$$

where

$$\Delta_m = \frac{1}{r}\frac{\partial}{\partial r}\left(r\frac{\partial}{\partial r}\right) + \frac{\partial^2}{\partial z^2} - \frac{m^2}{r^2}\,, \qquad \mathcal{L}_m = \Delta_m - \frac{1}{r^2}\,. \tag{3.32}$$

Eliminating all variables except w_m yields a basic equation to be solved :

$$\Delta_m \frac{\partial^2 \tilde{w}_m}{\partial z^2} = h\left[m^2 \Delta_m w_m - r\,\mathcal{L}_m\left(r\frac{\partial w_m}{\partial z}\right)\right], \tag{3.33}$$

which is essentially same as (4.8) in Matsuda, Sakurai and Takeda (1975).

3.2 Boundary conditions

The configuration of the cylinder is the same as that of incompressible case, which has the flat top cover at $z = H_0$ and the bottom shape given by (2.3).

The boundary condition at the top is nothing but a compressible version of the Ekman compatibility condition (Landahl 1977), and is

$$\tilde{w}_0 = -\frac{E^{\frac{1}{2}}}{2r\epsilon_R}\frac{\partial}{\partial r}\left[(1+hr^2)^{\frac{1}{4}} r\,\epsilon_R^{\frac{1}{2}}(v_0 - r)\right] \qquad \text{at } z = H_0\,, \tag{3.34a}$$

$$w_m = -\frac{E^{\frac{1}{2}}}{2r\epsilon_R}\frac{\partial}{\partial r}\left[(1+hr^2)^{\frac{1}{4}} r\,\epsilon_R^{\frac{1}{2}}\, v_m\right] \qquad \text{at } z = H_0\,. \tag{3.34b}$$

$$(m = 1, 2, \cdots)$$

As the boundary condition at the bottom, we use the Ekman compatibility condition applied on a slightly inclined surface, such as the case of the incompressible fluid :

$$\frac{1}{|m^*|}(\zeta \cdot m^*) = \frac{E^{\frac{1}{2}}}{2r\epsilon_R}\frac{\partial}{\partial r}\left[(1+hr^2)^{\frac{1}{4}} \cdot r \cdot \epsilon_R^{\frac{1}{2}} \cdot (\zeta \cdot e_\theta^*)\right], \tag{3.35}$$

where m^* is given by (2.6) and e_θ^* is a unit vector perpendicular to the radial vector and lies on the surface. Substitution of (2.6) into (3.35) gives

$$-v_I F \sum_{m=1}^{m} \frac{h_m}{r} im e^{im\theta} + w_I = \frac{E^{\frac{1}{2}}}{2r\epsilon_R}\frac{\partial}{\partial r}\left[(1+hr^2)^{\frac{1}{4}} r \epsilon_R^{\frac{1}{2}} v_I\right] \tag{3.36}$$

$$\text{at} \quad z = 0 ,$$

where the bottom condition is applied at $z = 0$ because of $F \ll 1$. The axisymmetric part of (3.36) is

$$w_0 = \frac{E^{\frac{1}{2}}}{2r\epsilon_R}\frac{\partial}{\partial r}\left[(1+hr^2)^{\frac{1}{4}} r \epsilon_R^{\frac{1}{2}} v_0\right] \qquad \text{at} \quad z = 0 , \tag{3.37}$$

and the non-axisymmetric component is

$$\begin{aligned} w_m = {} & \frac{iF}{r}\left[m v_0 h_m + (m-1) v_1 h_{m-1} + \cdots + v_{m-1} h_1\right] \\ & + \frac{E^{\frac{1}{2}}}{2r\epsilon_R}\frac{\partial}{\partial r}\left[(1+hr^2)^{\frac{1}{4}} r \epsilon_R^{\frac{1}{2}} v_m\right] \qquad \text{at} \quad z = 0 . \end{aligned} \tag{3.38}$$

The boundary condition for w_m will be given after the solutions $v_0, v_1, - - - , v_{m-1}$ are determined. We need one more boundary

condition at the top and the bottom, since (3.33) is fourth order with respect to z. This boundary condition is derived from (3.26 and is

$$\frac{\partial w_m}{\partial z} = 0 \qquad \text{at } z = H_c \quad \text{and} \quad z = 0 . \tag{3.39}$$

On the side wall we require

$$w_m = 0 \qquad \text{at} \quad r = 1 , \tag{3.40}$$

which leads to $v_m = T_m = 0$. Because u_m is of higher order with respect to E, the boundary condition for u_m is ajusted by higher order boundary layers.

3.3 Solution

It is possible to solve (3.33) under the boundary conditions (3.34b), (3.38), (3.39), and (3.40). But, since it is very complicated to solve a general case, let us restrict ourselves to a simple configuration such as the Pedlosky & Greenspan type cylinder with a sloping flat bottom. In this case the bottom geometry is expressed as

$$z = F r e^{i\theta} . \tag{3.41}$$

The non-axisymmetric boundary condition (3.38) reduces to

$$w_1 = i F v_0 + \frac{E^{\frac{1}{2}}}{2 r \epsilon_R} \frac{\partial}{\partial r} \left[(1+hr^2)^{\frac{1}{4}} r \epsilon_R^{\frac{1}{2}} v_1 \right] . \tag{3.42}$$

The axisymmetric part of the solution is easily obtained. Since w_0 is independent of z from (3.19), we can equate (3.34a) and (3.37) and obtain

$$w_0 = \frac{E^{\frac{1}{2}}}{4r\epsilon_R} \frac{d}{dr} \left[(1+hr^2)^{\frac{1}{4}} r^2 \epsilon_R^{\frac{1}{2}} \right] . \tag{3.43}$$

And the azimuthal component v_0 is

$$v_0 = \frac{r}{2} . \tag{3.44}$$

Assuming $E^{\frac{1}{2}} \ll F \ll 1$, the order of magnitude of w_1 should be F from (3.42). A careful inspection of equations from (3.26) to (3.31) shows that all variables, i.e. u_m, v_m, w_m, T_m, ρ_m and p_m, have the same order of magnitude. Therefore in the lowest order the boundary condition (3.42) can be written as

$$w_1 = i F v_0 = \frac{1}{2} i F r \qquad \text{at} \quad z = 0 . \tag{3.45}$$

The condition (3.34b) is approximated as

$$w_1 = 0 \qquad \text{at} \quad z = H_0 . \tag{3.46}$$

Now the problem is to solve (3.33) under the boundary conditions (3.39), (3.40), (3.45) and (3.46). If the non-dimensional parameter h is small, the solution may be expanded in terms of h :

$$\tilde{w}_1 = \tilde{w}_1^{(0)} + h\,\tilde{w}_1^{(1)} + \cdots \quad . \tag{3.47}$$

Substitution of (3.47) into (3.33) for m = 1 gives the lowest order equation :

$$\Delta_1 \frac{\partial^2 \tilde{w}_1^{(0)}}{\partial z^2} = 0 \quad . \tag{3.48}$$

We only show the zeroth order solution here.

$$v^{(0)} = \frac{r}{2} - \frac{F}{2} r\cos\theta \sum_{n=1}^{\infty} \frac{J_1(\lambda_n r)}{J_2(\lambda_n)\left[\sinh\lambda_n H_0 - \frac{H_0}{2}\lambda_n (1+\cosh\lambda_n H_0)\right]}$$
$$\times \left[1+\cosh\lambda_n H_0 - \cosh\lambda_n z - \cosh\lambda_n (z-H_0)\right] , \tag{3.49}$$

$$w^{(0)} = \frac{E^{\frac{1}{2}}}{\delta \epsilon_R^{\frac{1}{2}}} (4 + G_0 r^2)$$
$$- \frac{F}{2}\sin\theta \left\{ \frac{r}{2} + \sum_{n=1}^{\infty} \frac{J_1(\lambda_n r)}{\lambda_n J_2(\lambda_n)\left[\sinh\lambda_n H_c - \frac{H_0}{2}\lambda_n (1+\cosh\lambda_n H_0)\right]} \right.$$
$$\left. \times \left[\lambda_n (z-\tfrac{H_c}{2})(1+\cosh\lambda_n H_c) - \sinh\lambda_n z - \sinh\lambda_n (z-H_c)\right] \right\} , \tag{3.50}$$

where λ_n is the n-th zero of Bessel function J_1.

3.4 Results

The results are explained as follows. In spite of the non-axisymmetric bottom shape, the axisymmetric geostrophic wind of the order unity v_0 can blow. This situation is very different

from the corresponding incompressible case in which no axisymmetric wind is induced in the lowest order. In the case of compressible fluid, particles of fluid can hardly move in the radial direction because of a stable stratification along a radial coordinate , and therefore the O(1) azimuthal velocity is permitted.

The geostrophic wind should flow along the bottom slope , and for this reason a z-motion w_1 of O(F) is induced. In the figure 8 this streamlines on the surface whose radial coordinate is constant (r = 0.5) is shown for $H_0 = 10$. The O(F) flow produced by the sloping bottom affects the flow field in the inner core via a viscous effect, and the azimuthal flow of O(F) is induced.

The conclusion drawn from these considerations is that the inner azimuthal flow is not affected in the lowest order by the geometry of the top/bottom if $F \ll 1$, while the flow along the cylinder axis is perturbed if $F \gg E^{\frac{1}{2}}$.

4. Conclusions

In the case of the incompressible fluid, flows are essentially two-dimensional even under non-axisymmetric circumstances such as in the present paper, because velocity components are independent of the axial coordinate due to the Taylor-Proudman theorem. So the bottom shape has a great influence on the flow pattern and magnitude. On the other hand the compressible fluid may have three-dimensional flow. In the rapidly rotating gas, the gas particles can hardly move in the radial direction because of the stable stratification, and the radial velocity is only of

O(E) . In this situation the O(1) azimuthal flow is allowed and the effect of a bottom shape on the flow is small in the case of $F \ll 1$.

Let's compare the fluid motion in the incompressible fluid with the compressible one in the case of the Pedlosky & Greenspan problem. Westward intensification is observed in the incompressible fluid. The flow in the inner core is weak and of the order of ε . On the other hand compressible fluid has an azimuthal flow of O(1) and has a weak three-dimensional axial motion due to the bottom shape. Moreover, in the lowest order these flows are confined to the surfaces whose radial coordinates are constant.

The authers wish to thank Dr. I. Hachisu for helpful discussions. The numerical calculations were performed on the FACOM M-200 at the Data Processing Center of Tyoto University.

References

Beardsley, R.C. 1969 A laboratory model of the wind-driven ocean circulation. J. Fluid Mech. 38, 225-271.

Charney, J. G. 1973 " Planetary fluid dynamics " in Dynamic Meteorology, ed. by P. Morel (D. Reidel Publishing Co., Dordrecht, Holland.), 97-351.

Cole, J. D. 1968 Purturbation Methods in Applied Mathematics. Chapter 4. London : Blaisdell.

Greenspan, H. P. 1968 The Theory of Rotating Fluids. Chapter 5. Cambridge University Press.

Kuo, H-H. & Veronis, G. 1971 The source-sink flow in a rotating system and its oceanic analogy. J. Fluid Mech. 45, 441-464.

Landahl, M. T. 1977 " Boundary layers and shear layers in a rapidly rotating gas " in Proceedings 2nd workshop on gases in strong rotation, ed. by Soubbaramayer, 15-50.

Matsuda, T., Sakurai, T. & Takeda, H. 1975 Source-sink flow in a gas centrifuge. J. Fluid Mech. 69, 197-208.

Matsuda, T. & Hashimoto, K. 1978a The structure of the Stewartson layers in a gas centrifuge. Part 1. Insulated end plates. J. Fluid Mech. 85, 433-442.

Matsuda, T. & Takeda, H. 1978b The structure of the Stewartson layers in a gas centrifuge. Part 2. Insulated side wall. J. Fluid Mech. 85,443-457.

Pedlosky, J. & Greenspan, H. P. 1967 A simple laboratory model for the oceanic circulation. J. Fluid Mech. 27, 291-304.

Stommel, H. 1948 The westward intensification of wind-driven ocean currents. Trans. Am. Geoph. Union, 29, 202-206.

Soubbaramayer 1979 " Centrifugation " in Uranium Enrichment, ed. by S. Villani (Springer-Verlag, Berlin), 183-244.

Figure caption

Figure 1. Configurations of (a) the cylinder with the off-axial paraboroidal bottom and (b) the cylinder with the sloping flat bottom.

Figure 2. Pressure isolines or streamlines of the steady driven flow of an incompressible fluid in the rotating cylinder whose bottom is the off-axial paraboroid ; $b = 1.5$ and $\varepsilon = 0.01$, the thick line shows a numerical solution and the thin one an analytic solution. $p_{min} = -0.0282$.

Figure 3. Pressure isolines ; $b = 0.05$ and $\varepsilon = 0.01$. $p_{min} = -0.498$.

Figure 4. Pressure isolines ; $b = 0.5$ and $\varepsilon = 0.01$. $p_{min} = -0.196$.

Figure 5. Pressure isolines ; $b = 0.7$ and $\varepsilon = 0.01$. $p_{min} = -0.102$.

Figure 6. Pressure isolines ; $b = 0.9$ and $\varepsilon = 0.01$. $p_{min} = -0.0578$.

Figure 7. Locus of the point of the minimum pressure with changing b.

Figure 8. Streamlines of the compressible fluid in the constant r section ($r = 0.5$). The flow of O(F) is induced by the sloping flat bottom.

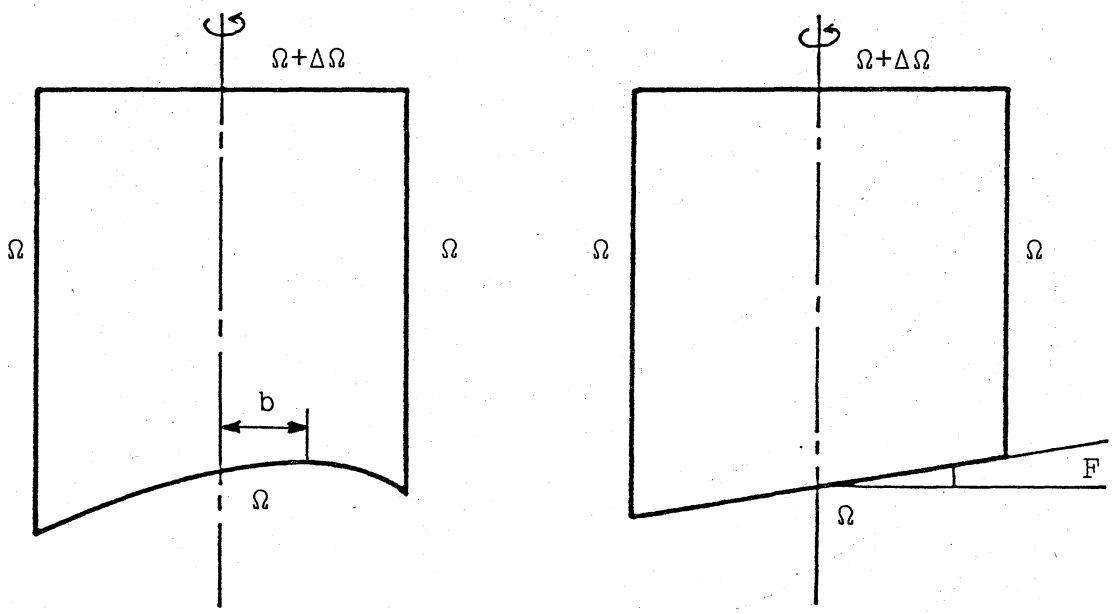

Figure 1.

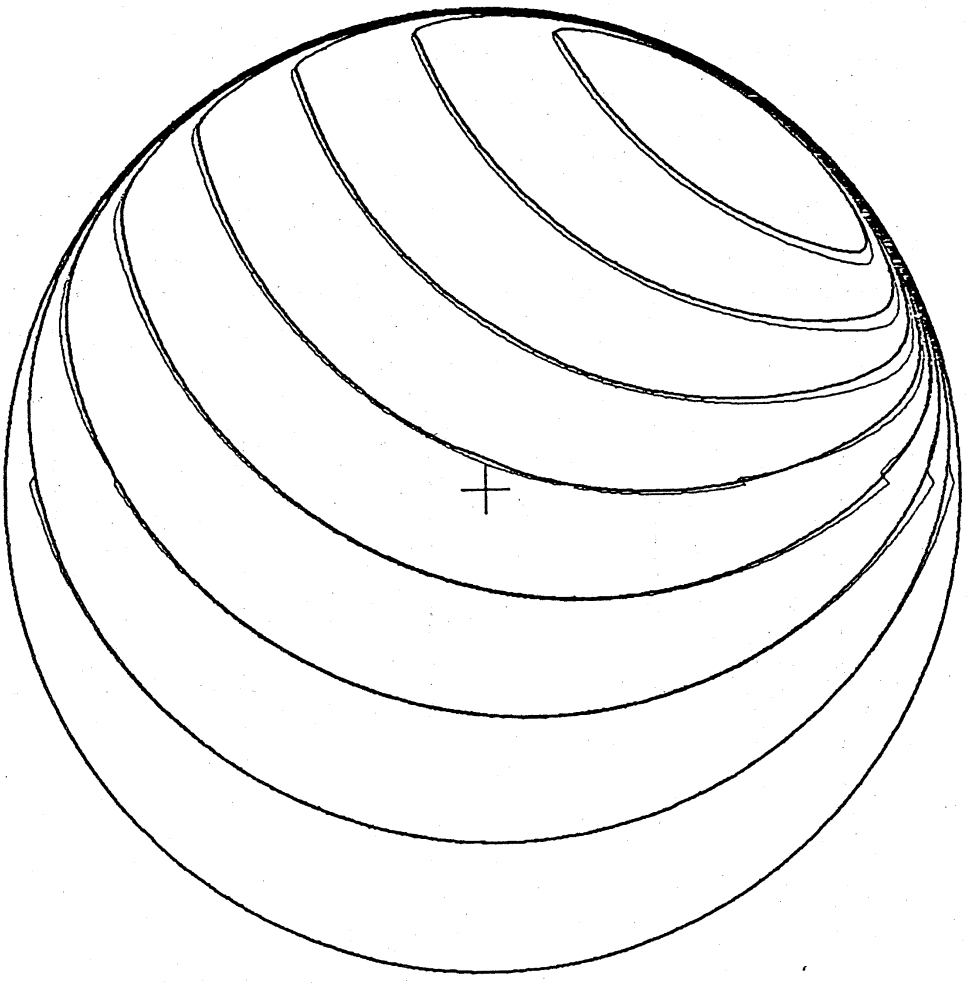

Figure 2.

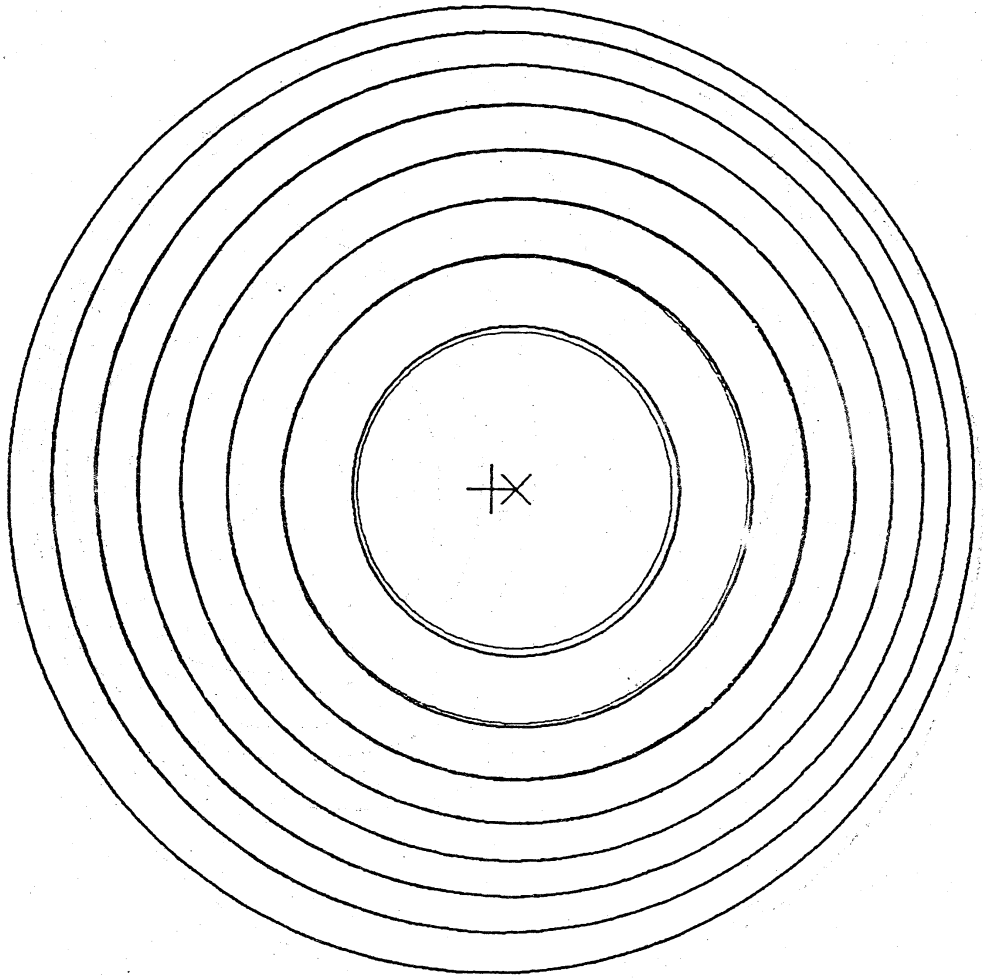

Figure 3.

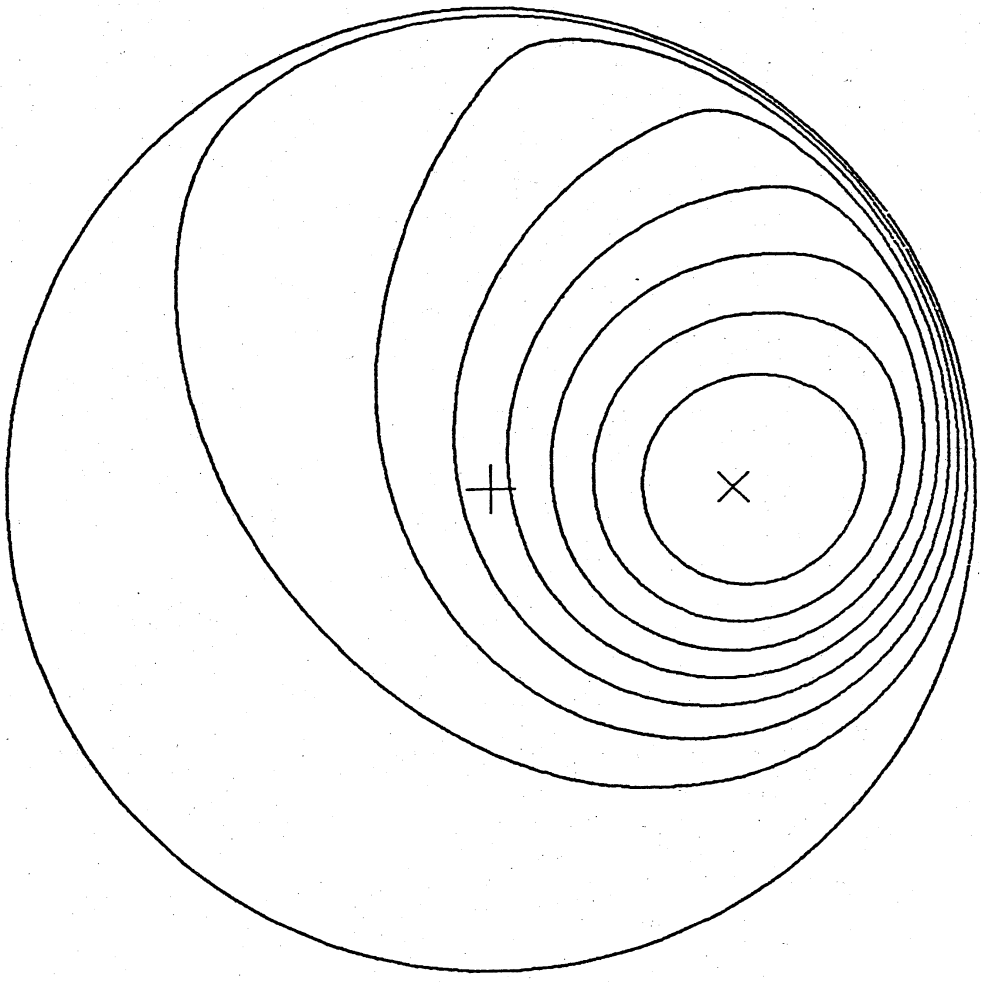

Figure 4.

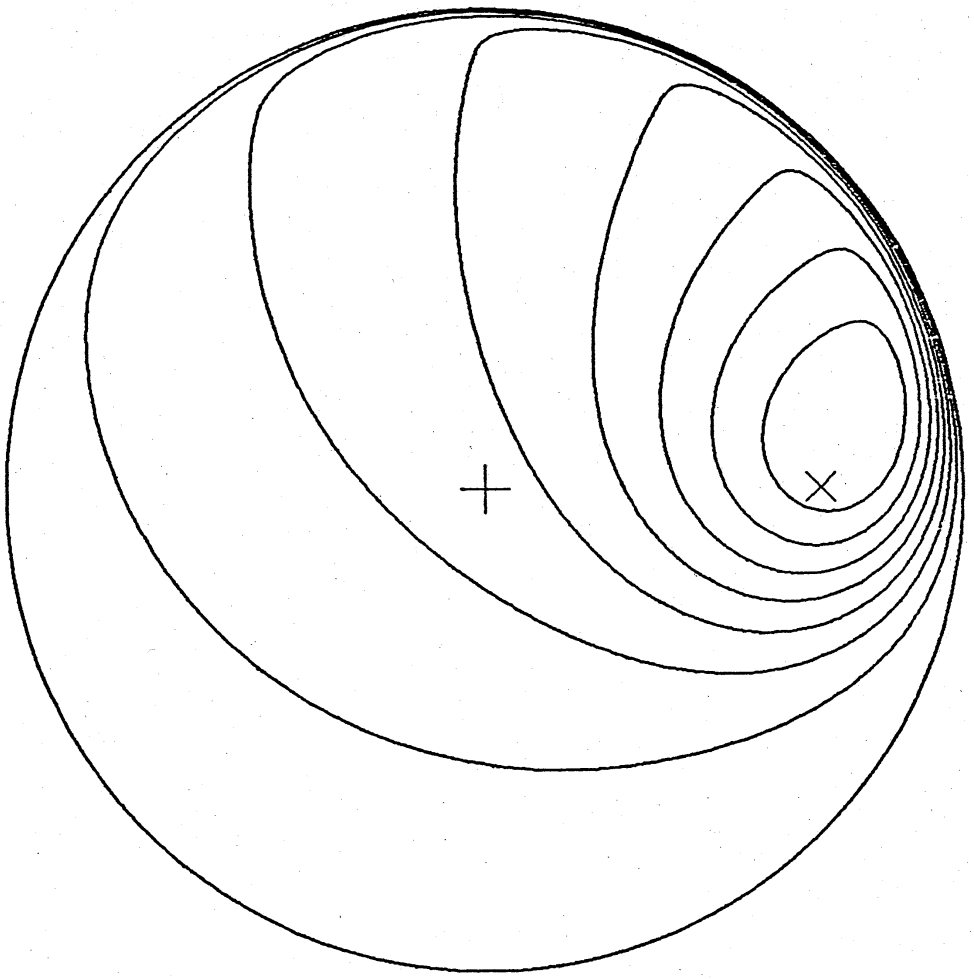

Figure 5.

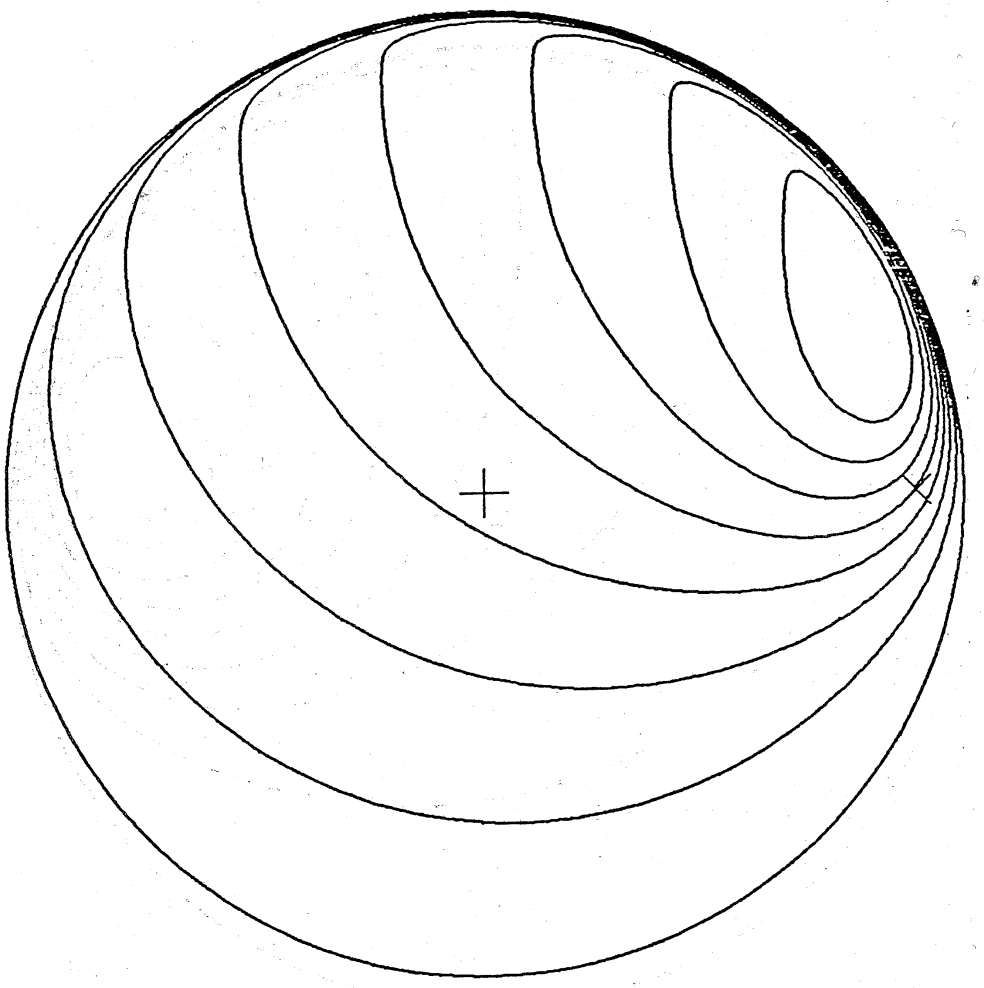

Figure 6.

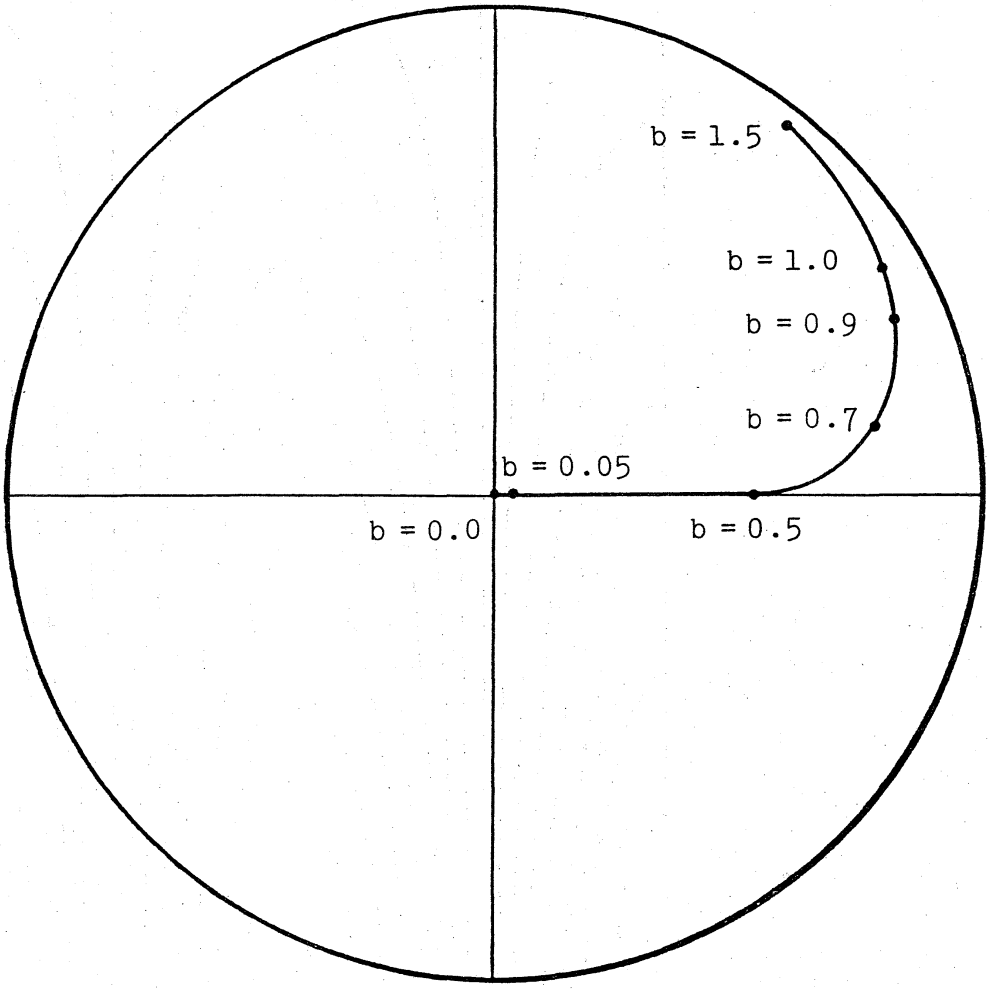

Figure 7.

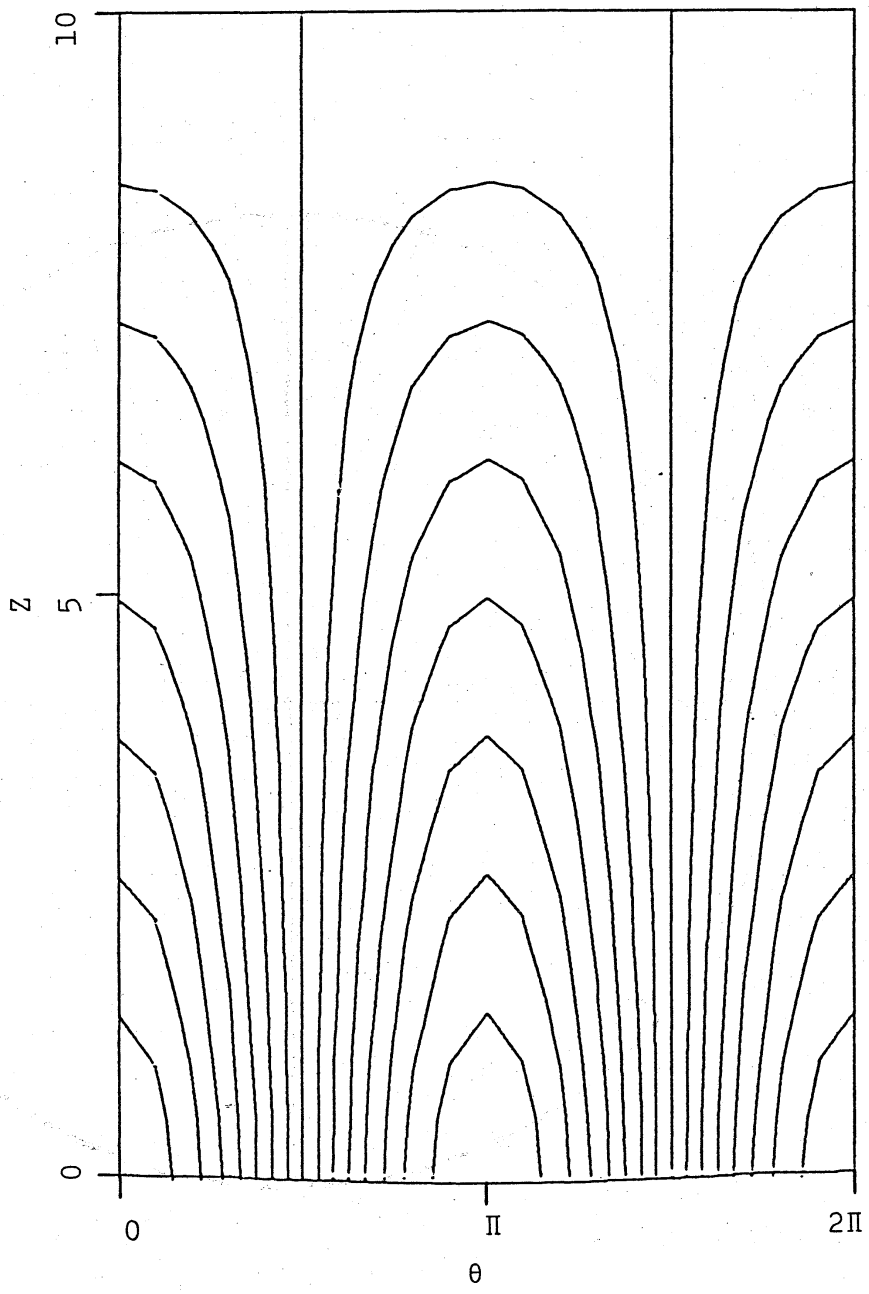

Figure 8.